



ELSEVIER

Contents lists available at ScienceDirect

## Surface &amp; Coatings Technology

journal homepage: [www.elsevier.com/locate/surfcoat](http://www.elsevier.com/locate/surfcoat)

# Study on thermoelectric property optimization of mixed-phase bismuth telluride thin films deposited by co-evaporation process

Yen-Ju Wu<sup>a,1</sup>, Shih-Chieh Hsu<sup>b,1</sup>, Ya-Cheng Lin<sup>c</sup>, Yibin Xu<sup>a</sup>, Tung-Han Chuang<sup>d,\*</sup>, Sheng-Chi Chen<sup>c,e,\*</sup>

<sup>a</sup> Center for Materials Research by Information Integration (CMI2), Research and Services Division of Materials Data and Integrated System (MaDIS), National Institute for Materials Science (NIMS), 1-1 Namiki, Tsukuba, Ibaraki 305-0044, Japan

<sup>b</sup> Department of Chemical and Materials Engineering, Tamkang University, New Taipei City 251, Taiwan

<sup>c</sup> Department of Materials Engineering and Center for Plasma and Thin Film Technologies, Ming Chi University of Technology, Taipei 243, Taiwan

<sup>d</sup> Institute of Materials Science and Engineering, National Taiwan University, Taipei 106, Taiwan

<sup>e</sup> College of Engineering, Chang Gung University, Taoyuan 333, Taiwan

## ARTICLE INFO

## Keywords:

Bi<sub>2</sub>Te<sub>3</sub>  
Thermoelectric properties  
Co-evaporation  
Thin films  
Mixed phases

## ABSTRACT

The development of Bi<sub>2</sub>Te<sub>3</sub> thin films has huge potential in the pursuit of efficient thermoelectric micro/nanodevices due to their high Seebeck coefficient, high electrical conductivity and low thermal conductivity. The optimization of experimental parameters of Bi-Te thin films produced by co-evaporation will be investigated in this study. Co-evaporation is a low cost, easy-to-control process which can be used for high throughput and is scalable. We found that an optimal Te/Bi ratio of 1.5 with good thermoelectric properties can be directly synthesized by Bi and Bi<sub>2</sub>Te<sub>3</sub> co-evaporation. Compared to the conventional Bi/Te co-evaporation process, high temperature annealing or substrate heating is not necessary for the process mentioned in this paper, which is a desirable feature when using polymer-based substrates, organic/inorganic hybrid thermoelectric generators, and flexible devices since they have relatively low tolerance to heat. The optimized Bi<sub>2</sub>Te<sub>3</sub> thin films, which are mixed phases of Bi<sub>2</sub>Te<sub>3</sub>, Bi<sub>3</sub>Te<sub>4</sub> and Te, possess high carrier concentration ( $6.65 \times 10^{20} \text{ cm}^{-3}$ ), low electrical resistivity ( $3.17 \times 10^{-3} \text{ } \Omega\text{cm}$ ), and extremely low thermal conductivity (0.59 W/mK) at room temperature on a smooth surface (roughness < 5.5 nm) and are achieved by adjusting the deposition rate of Bi and Bi<sub>2</sub>Te<sub>3</sub>. The correlation between the structures of mixed phases, electrical and thermal properties will be discussed in detail.

## 1. Introduction

Thermoelectric materials require a high figure-of-merit  $ZT$  [ $ZT = (S^2\sigma/\kappa)T$ ] for high efficiency and performance; i.e. the materials need to exhibit high Seebeck coefficient ( $S$ ), high electrical conductivity ( $\sigma$ ) and low thermal conductivity ( $\kappa$ ). Bi<sub>2</sub>Te<sub>3</sub>, a narrow-gap semiconductor of 0.15 eV with a rhombohedral unit cell of space group R $\bar{3}m$  [1], is a well-established thermoelectric material because of its good thermoelectric properties ( $ZT \approx 1$ ). The unit cell is composed of five atomic layers of Te<sup>1</sup>-Bi<sup>1</sup>-Te<sup>2</sup>-Bi<sup>1</sup>-Te<sup>1</sup>, which stacked by Van der Waals along the  $c$ -axis [1,2]. This structural characterization can effectively hinder the phonon transport in the materials.

Thin films technology is desirable in the production of efficient integrated thermoelectric devices especially for thermoelectric micro-generation. In order to scale the bulk of thermoelectric devices down to

the nano/micron-size scale, several deposition techniques have been reported in literature for the fabrication of Bi<sub>2</sub>Te<sub>3</sub> thin films; for example, metal-organic chemical vapor deposition [3–5], co-sputtering [6–8], evaporation [9,10] and electrochemical deposition [11]. Tan et al. reported the improvement of thermoelectric properties of  $n$ -Bi<sub>2</sub>Se<sub>0.5</sub>Te<sub>2.5</sub> and  $p$ -(Bi<sub>0.5</sub>Sb<sub>0.5</sub>)<sub>2</sub>Te<sub>3</sub> pillar array films produced by ion-beam-assisted sputtering [12,13]. They used this method to fabricate  $n$ -type Bi<sub>2</sub>Te<sub>3</sub>/ZrB<sub>2</sub> superlattice films in order to further enhance the  $ZT$  [14]. Pires et al. also prepared Bi-Te thin films by adjusting the ion beam sputtering and analyzing the beam voltage impact on the thermoelectric performance [15]. Zhou et al. deposited and optimized thermoelectric properties of the  $n$ -type Pb-doped Bi<sub>2</sub>Te<sub>3</sub> thin films by radio frequency magnetron sputtering [16]. Lal et al. reported on the optimization of annealing conditions for  $p$ -type BiSbTe thin films using pulse electrodeposition [11]. Sudarshan et al. noted the change from

\* Corresponding authors.

E-mail addresses: [tunghan@ntu.edu.tw](mailto:tunghan@ntu.edu.tw) (T.-H. Chuang), [chensc@mail.mcut.edu.tw](mailto:chensc@mail.mcut.edu.tw) (S.-C. Chen).

<sup>1</sup> These authors contributed equally to this work.

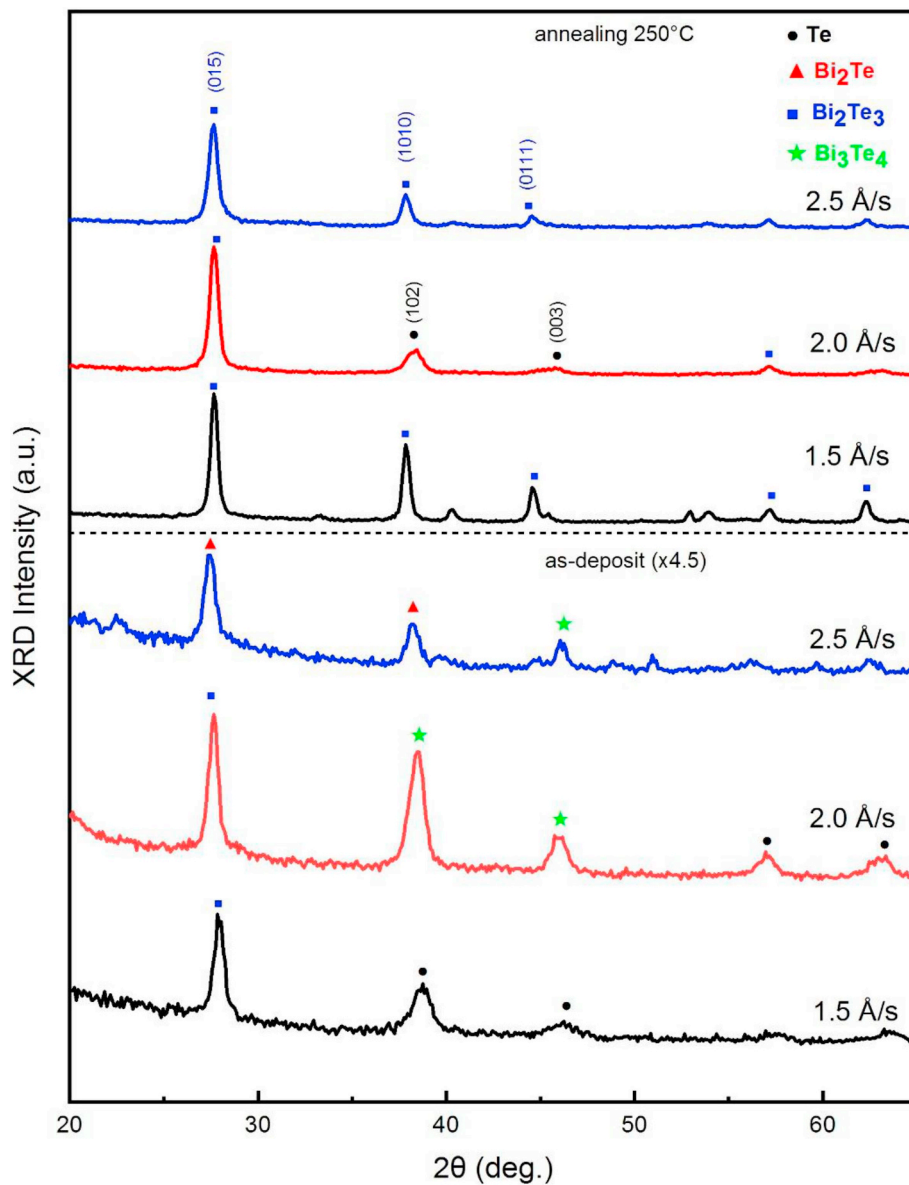


**Fig. 1.** XRD of bismuth telluride thin films deposited with various Bi-deposition rate of 1.5 (blue), 2.0 (red) and 2.5 (black) Å/s. Top are thin films with 250 °C annealing and the bottom are as-deposited thin films. (For interpretation of the references to colour in this figure legend, the reader is referred to the web version of this article.)

semiconductor to metallic behavior of e-beam evaporated  $\text{Bi}_2\text{Te}_3$  thin films through vacuum annealing [17]. Goncalves et al. deposited  $\text{Bi}_2\text{Te}_3$  thin films by the thermal co-evaporation of Te and Bi targets [9]. The contributions on the control of the compositions and phases are reported as well via various techniques. Nuthongkum et al. investigated the structures effect in  $\text{Bi}_x\text{Te}_y$  by changing the sputtering pressures via RF magnetron sputtering [18]. Concepcion et al. controlled the epitaxial growth of various Bi-Te phases by tuning the Nitrogen gas flow via physical vapor transport [2]. The temperature and the Bi/Te ratio are used to control various Bi-Te systems via metal-organic vapor-phase epitaxy by Kuznetsov et al. [19] Attila et al. reported a phase transition from  $\text{Bi}_4\text{Te}_3$  to  $\text{Bi}_2\text{Te}_3$  by tuning the Bi/Te ratio of molecular beam epitaxy [20]. Detailed analyses of thermoelectric thin-films can be found elsewhere [21–23].

In the present work the thermal evaporation method was chosen due to its scalability, relative simplicity and ease of control. We found the direct evaporation of a single  $\text{Bi}_2\text{Te}_3$  target results in thin films that are predominantly Te instead of the desired  $\text{Bi}_2\text{Te}_3$  thin films due to the large difference in the vapor pressures of Bi and Te. Goncalves et al. also

reported similar results of a compositional gradient through the thickness of films produced by single-target evaporation [9]. Therefore, we used  $\text{Bi}_2\text{Te}_3$  and Bi as the two targets in the film preparation using co-evaporation. From the literatures of  $\text{Bi}_2\text{Te}_3$  thin film fabrication including the abovementioned methods, high-temperature heat treatment during deposition or annealing is necessary to achieve good thermoelectric properties. To the best of our knowledge, little attention has been paid to low-temperature fabrication, which is important for wearable or flexible thermoelectric devices. These devices usually have low tolerance to high temperatures. We were able to produce  $\text{Bi}_2\text{Te}_3$  thin films possessing good thermoelectric properties through co-evaporation of Bi and  $\text{Bi}_2\text{Te}_3$ , with no further heat treatment necessary. This simple and easy procedure is attractive in the preparation of unique integrated thermoelectric microdevices. Moreover, the optimized parameters as well as insights into the relationship between mixed phases and film properties was also investigated.

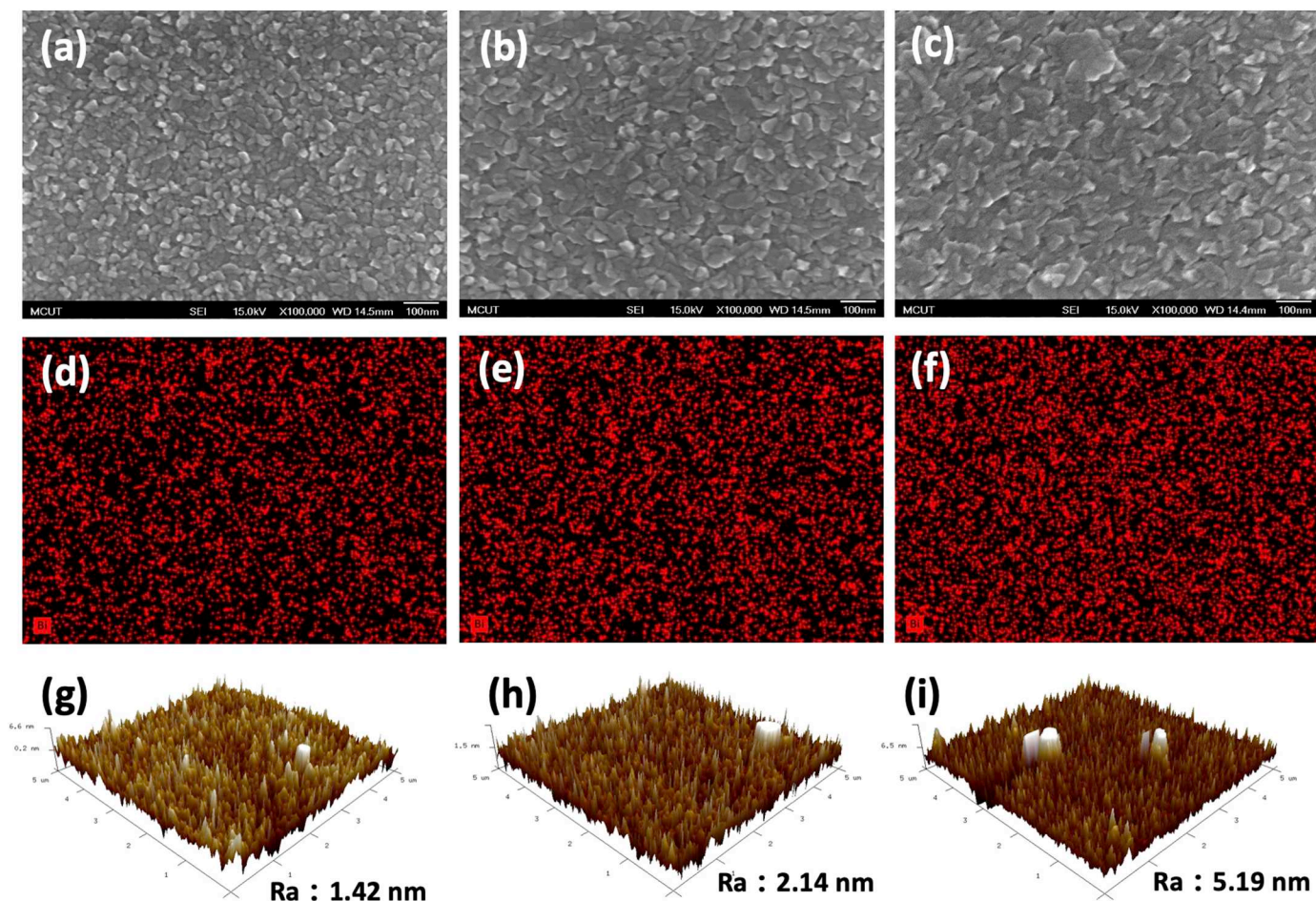


Fig. 2. The SEM, EDS of Bi and AFM analysis are shown in three rows from top to bottom, respectively. The samples deposited via various Bi-deposition rate of 1.5 Å/s (a, d, g), 2.0 Å/s (b, e, h) and 3 Å/s (c, f, i) are listed from left to right. The scale bars of SEM and EDS are the same at the right bottom in each SEM images.

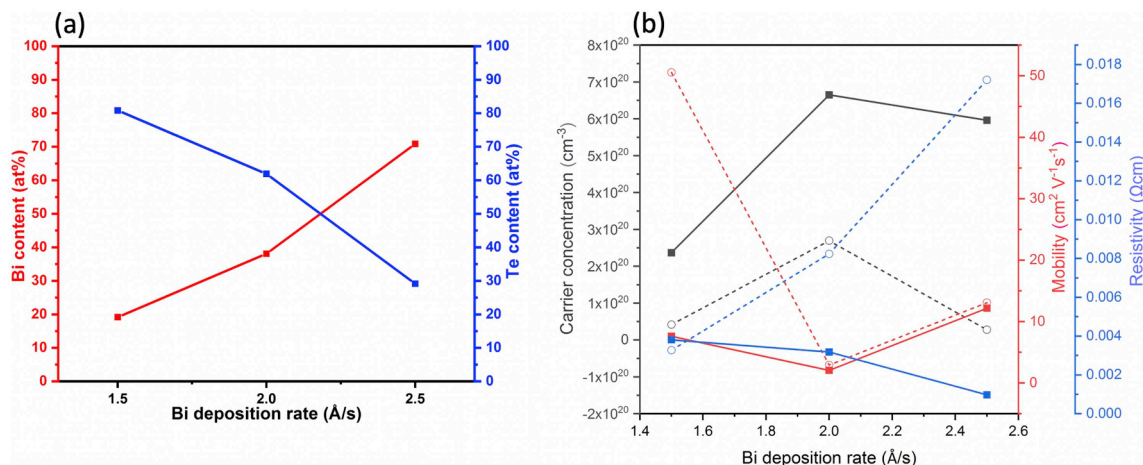


Fig. 3. (a) EPMA composition analysis and (b) electrical analysis of bismuth telluride thin films deposited with various Bi-deposition rate of 1.5, 2.0 and 2.5 Å/s. The solid line in (b) is represented as as-deposited thin films and dashed line are represented as 250 °C-annealed thin films.

## 2. Experimental procedure

The Bi<sub>2</sub>Te<sub>3</sub> thin films were deposited on Corning 1737F glass and Si substrates via co-evaporation by Bi and Bi<sub>2</sub>Te<sub>3</sub> targets in a pure Ar atmosphere with flow ratio of 5 sccm at ambient temperature. The substrates were cleaned using deionized water and acetone in an ultrasonic cleaner for 15 min prior to deposition. The background pressure and working pressure for the evaporation were  $<6 \times 10^{-6}$  Torr and

$1.5 \times 10^{-4}$  Torr, respectively. The rotation of the substrate holder was kept at 10 rpm. The deposition rate of Bi<sub>2</sub>Te<sub>3</sub> was fixed at 3 Å/s and Bi was in the range of 1.5 to 2.5 Å/s. Some of the resulting films were annealed at 250 °C in an Ar atmosphere for 1 h for the purpose of comparison with as-deposited thin films.

The crystal structure of the various Bi<sub>2</sub>Te<sub>3</sub> thin films was examined by X-ray diffraction (XRD) using Cu-K $\alpha$  radiation. The surface morphologies and roughness were analyzed by an atomic force



**Table 1**

The carrier concentration, mobility, resistivity, conductivity, roughness, thermal resistance, and (cross-plane) thermal conductivity of bismuth telluride thin films deposited via co-evaporation with various Bi-deposition rate. The sample 1 to 3 are as-deposited thin films and samples 3–6 are the annealed thin films.

Sample	Bi deposition rate ( $\text{\AA}/\text{s}$ )	$\text{Bi}_2\text{Te}_3$ deposition rate ( $\text{\AA}/\text{s}$ )	Annealing ( $^\circ\text{C}$ )	Carrier concentration ( $\text{cm}^{-3}$ )	Mobility ( $\text{cm}^2 \text{V}^{-1} \text{s}^{-1}$ )	Resistivity ( $\Omega\text{cm}$ )	Conductivity ( $\text{Scm}^{-1}$ )	Roughness (nm)	Thermal Resistance ( $10^{-9} \text{m}^2\text{K}/\text{W}$ ), $\perp$	Thermal conductivity ( $\text{W}/\text{mK}$ ), $\perp$
1	1.5	3		$2.36\text{E}+20$	7.58	$3.81\text{E}-03$	$2.62\text{E}+02$	1.42	$272.6 \pm 5.45$	0.726
2	2	3		$6.65\text{E}+20$	2.05	$3.17\text{E}-03$	$3.15\text{E}+02$	2.14	$471.3 \pm 14.65$	0.586
3	2.5	3		$5.96\text{E}+20$	12.17	$9.69\text{E}-04$	$1.03\text{E}+03$	5.19	$337.1 \pm 7.48$	1.020
4	1.5	3	250	$4.16\text{E}+19$	50.54	$3.27\text{E}-03$	$3.07\text{E}+02$	1.42	$254.8 \pm 6.29$	0.777
5	2	3	250	$2.69\text{E}+20$	2.92	$8.23\text{E}-03$	$1.21\text{E}+02$	2.14	$507.1 \pm 8.93$	0.544
6	2.5	3	250	$2.79\text{E}+19$	13.06	$1.72\text{E}-02$	$5.81\text{E}+01$	5.19	$257.4 \pm 7.89$	1.336

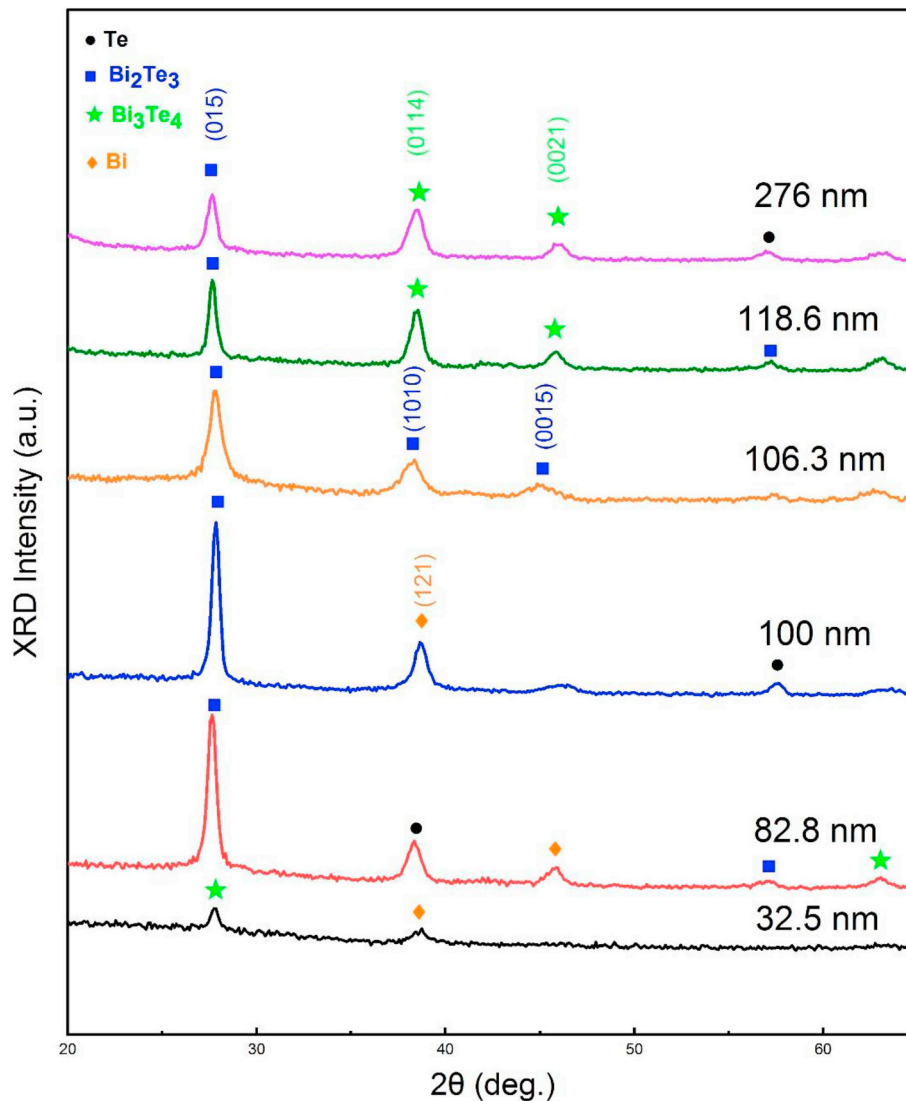


Fig. 4. XRD of bismuth telluride thin films with Bi-deposition rate of  $2.0 \text{\AA}/\text{s}$  of various thickness.

microscope (AFM) and Scanning Electron Microscope (SEM). The chemical composition and Bi distribution of the  $\text{Bi}_2\text{Te}_3$  thin films was analyzed using energy dispersive spectrometry (EDS) and electron probe X-ray microanalyzer (EPMA). The thicknesses of the films were measured by  $\alpha$ -step. The electrical properties were measured by the four-point probe and Hall measurement system. For the thermal measurement, the  $\text{Bi}_2\text{Te}_3$  thin films can directly perform as the heat transducer. The thermal conductivity along the cross-plane was characterized by the frequency-domain thermoreflectance (FDTR) [24], where three positions in each sample were measured at four different frequencies at

room temperature.

### 3. Results and discussion

The XRD results of bismuth telluride thin films deposited via co-evaporation at various Bi-deposition rates are shown in Fig. 1. The results from as-deposited thin films (the peak intensity was multiplied by 4.5) and  $250^\circ\text{C}$ -annealed thin films are shown in the bottom and top, respectively. The crystallinity of all samples was improved while the phase composition has no obvious tendency after the annealing. The

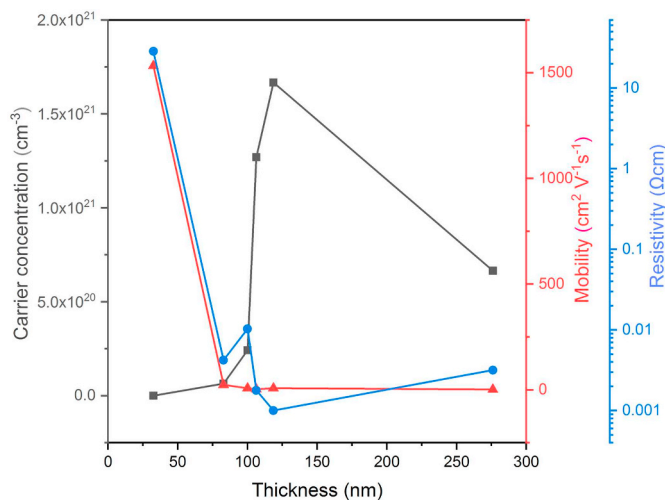


Fig. 5. Electrical analysis of bismuth telluride thin films with Bi-deposition rate of 2.0 Å/s versus various thickness.

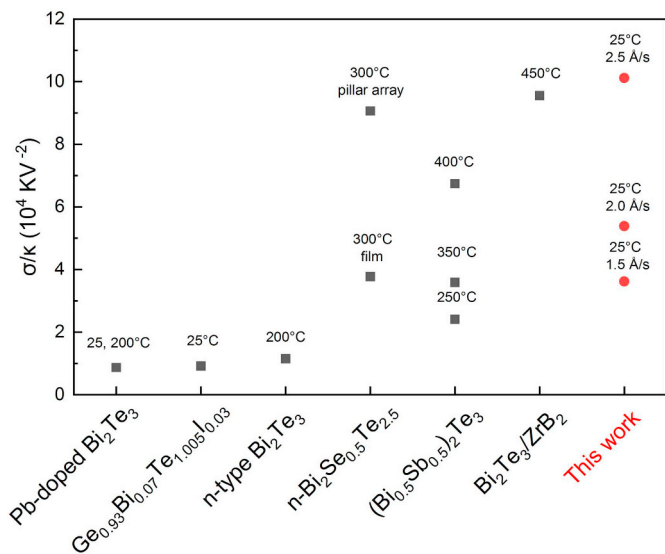


Fig. 6. Comparison of the ratio of electrical conductivity and thermal conductivity ( $\sigma/\kappa$ ) with various reported Bi-Te based materials, Pb-dope Bi<sub>2</sub>Te<sub>3</sub> [16], Ge<sub>0.93</sub>Bi<sub>0.07</sub>Te<sub>1.005</sub>I<sub>0.03</sub> [26], n-type Bi<sub>2</sub>Te<sub>3</sub> [25], n-Bi<sub>2</sub>Se<sub>0.5</sub>Te<sub>2.5</sub> [12], (Bi<sub>0.5</sub>Sb<sub>0.5</sub>)<sub>2</sub>Te<sub>3</sub> [13], Bi<sub>2</sub>Te<sub>3</sub>/ZrB<sub>2</sub> [14], and our bismuth telluride thin films deposited with various Bi-deposition rate of 1.5, 2.0 and 2.5 Å/s.

dominant XRD peak in most samples can be characterized as being Bi<sub>2</sub>Te<sub>3</sub> phase. When the Bi-deposition rate is increased, the mixed phases of as-deposited thin films change from lower Bi/Te phase (Bi<sub>3</sub>Te<sub>4</sub>, Te; Bi<sub>2</sub>Te<sub>3</sub>, Bi<sub>3</sub>Te<sub>4</sub>), to higher Bi/Te phase (Bi<sub>2</sub>Te, Bi<sub>3</sub>Te<sub>4</sub>). Usually, the most stable mixed phases will remain after deposition. This indicates that the most stable mixed phases will change and are strongly affected by the Bi-deposition rate which provides different Bi/Te ion ratios during deposition. Fig. 2 shows the SEM, EDS of Bi and AFM analyses of the films. The particle size of the film surface increases from around 32 nm at 1.5 Å/s to 48 nm and 64 nm as the Bi-deposition rate increases to 2.0 and 2.5 Å/s respectively, as shown in Fig. 2(a), (b) and (c). The Bi distribution also increases corresponding to the increase of the Bi-deposition rate as shown in Fig. 2(d), (e) and (f). The film roughness is <5.5 nm in all samples, as characterized by AFM. The roughness of the three samples are 1.42 nm, 2.14 nm, and 5.19 nm, respectively, as shown in Fig. 2(g), (h) and (i).

The Bi/Te atomic ratio increases upon increasing the Bi-deposition rate as shown in Fig. 3(a). The sample deposited at a Bi-deposition rate

of 2.0 Å/s has an atomic ratio close to Bi<sub>2</sub>Te<sub>3</sub>. However, the crystalline structures are mixed phases composed of Bi<sub>2</sub>Te<sub>3</sub>, Bi<sub>3</sub>Te<sub>4</sub>, and Te as shown in Fig. 1. This implies that the structures of deposited thin films do not only rely on the atomic ratio of Bi/Te but are also dependent upon the morphology, especially for the mixed phase thin films. From the carrier concentration, mobility and resistivity results in Fig. 3(b), we can see the as-deposited thin films have similar or even lower electrical resistivity than the annealed thin films. Hall measurement shows all samples possess n-type conduction. The carrier concentration decreases significantly while the mobility does not change as much for the samples of 2.0 Å/s and 2.5 Å/s after annealing. The conductivity ( $\sigma$ ) can be calculated using  $\sigma = 1/R = ne\mu_e$ , where the  $\sigma$  is electrical conductivity,  $R$  is electrical resistivity,  $n$  is carrier concentration, and  $\mu_e$  is electrical mobility. The electrical conductivity of the as-deposited films increases as the Bi-deposition rate rises, which correlates to the increase in particle size (as shown in the SEM results in Fig. 2) and the composition change. Nevertheless, the electrical conductivity does not improve after annealing, which could be attributable to the restriction of grain growth by the mixed phases. The calculated grain size from the dominant peak of XRD is around 12.6–13.7 nm in the as-deposited films, and 12.4–16.6 nm in the annealed films, in reasonable agreement with the restriction of grain size after annealing.

The details of measured electrical and thermal properties of the bismuth telluride thin films deposited at various Bi-deposition rates are listed in Table 1. The results indicate that as-deposited films can achieve similar thermoelectric properties compared with the annealed films. The thin film with a Bi-deposition rate of 2.0 Å/s has the lowest cross-plane thermal conductivity of 0.586 W/mK, which is quite low compared to other Bi-Te based thin films [12–14,16,25,26]. Moreover, the thermal conductivity changes least after annealing which might be attributable to the limitation of grain growth by the multi-phases co-existing in the films. The as-deposited thin film (sample 2) with a Bi-deposition rate of 2.0 Å/s is the optimal sample due to its very low thermal conductivity and good electrical conductivity. Our results show that good thermoelectric properties can be achieved without the need for annealing or substrate heating via Bi and Bi<sub>2</sub>Te<sub>3</sub> co-evaporation. This film is composed of mixed phases of Bi<sub>2</sub>Te<sub>3</sub>, Bi<sub>3</sub>Te<sub>4</sub>, and Te, which indicates that phonon transport can be effectively hindered by the interfaces of the various phases. In this study, the Bi<sub>2</sub>Te<sub>3</sub>, Bi<sub>3</sub>Te<sub>4</sub> and Te can be tuned through the deposition rates of Bi and Bi<sub>2</sub>Te<sub>3</sub>: As the Bi deposition rate rises, the Bi<sub>2</sub>Te and Bi<sub>3</sub>Te<sub>4</sub> phases increase; As the Bi deposition rate drops, the Te and Bi<sub>2</sub>Te<sub>3</sub> phases increase. Goto et al. also proposed a low thermal conductivity at around 0.5 W/mK in Bi-Te films which are composed of multi-phases (Bi<sub>4</sub>Te<sub>3</sub>, Bi<sub>2</sub>Te and Bi<sub>3</sub>Te<sub>7</sub>) by combinatorial sputter coating technology [27], in reasonable agreement with our results. The phonon scattering at the interfaces between dissimilar phases including the crystallographic mis-orientation, differential acoustic scattering and the grain size effect on thermal conductivity in polycrystalline materials contribute to the low thermal conductivity [28]. The discussion on thermal conductivity of multi-phase materials that incorporates equation derivation can be found elsewhere [29,30].

In order to understand the effects of the film thickness on the structure and transport properties, films with a Bi-deposition rate of 2.0 Å/s were deposited into various thicknesses from 32.5 nm to 276 nm for XRD analysis as shown in Fig. 4. With the exception of the 32.5 nm film, the dominant XRD peak of all other films can be characterized as Bi<sub>2</sub>Te<sub>3</sub> phase. The thinnest film (32.5 nm) also has low crystallinity while the other films have clear crystallinity peaks. Upon increasing the film thickness, the mixed phases change from Bi<sub>2</sub>Te<sub>3</sub>, Te, Bi phases to Bi<sub>2</sub>Te<sub>3</sub>, Bi<sub>3</sub>Te<sub>4</sub>, Te phases. When the thickness rises above 110 nm, the composition of the mixed phases does not change. The measured electrical properties of these bismuth telluride films versus various thicknesses can be seen in Fig. 5. The carrier concentration has an inflection point at a thickness of 100 nm and mobility and resistivity show no significant change (2 to 7 cm<sup>2</sup> V<sup>-1</sup> s<sup>-1</sup>; 0.001 to 0.01 Ωcm)

above 100 nm. The best electrical conductivity of  $1.03 \times 10^3 \text{ Scm}^{-1}$  is achieved at 118 nm. This indicates that the optimal thin films possessing low thermal conductivity and good electrical conductivity can be achieved at a  $\text{Bi}_2\text{Te}_3$ -deposition rate of  $3.0 \text{ \AA/s}$  and Bi-deposition rate of  $2.0 \text{ \AA/s}$  with a thickness above 100 nm.

The ratio of electrical conductivity to thermal conductivity ( $\sigma/\kappa$ ) is an important factor in evaluating the thermoelectric performance. The  $\sigma/\kappa$  ratio of various reported Bi-Te based materials are compared with our as-deposited films in Fig. 6. Without annealing treatment, the reported  $\sigma/\kappa$  values are quite low at around  $8.6 \times 10^3 \text{ KV}^{-2}$ . However, the  $\sigma/\kappa$  of our as-deposited films is the highest, even higher than the reported annealed thin films such as  $\text{Bi}_2\text{Te}_3/\text{ZrB}_2$  superlattice thin films [14]. We have developed a simple and annealing-free method to produce mixed-phase bismuth telluride thin films for thermoelectric applications. This room temperature annealing-free process is beneficial and desirable for wearable devices which usually have an inability to handle high temperatures.

#### 4. Conclusion

Integrated flexible thermoelectric microdevices usually have low melting point and low tolerance to heat. We developed a low cost, annealing-free co-evaporation method for producing bismuth telluride thin films using Bi and  $\text{Bi}_2\text{Te}_3$  targets. Compared to the usual Bi/Te co-evaporation methods, which require heat treatment during deposition or further annealing, the proposed method in the present study is beneficial for wearable thermoelectric microdevices. We optimized the thermoelectric properties of the bismuth telluride thin films by adjusting the Bi and  $\text{Bi}_2\text{Te}_3$  deposition rates. We found that the Te/Bi ratio, thickness, and composition of mixed phases all affect the thermoelectric properties. The mixed phases of the optimized films are composed of  $\text{Bi}_2\text{Te}_3$ ,  $\text{Bi}_3\text{Te}_4$ , and Te and have Te/Bi atomic ratio of 1.5. The interfaces of various phases in the thin films can effectively hinder phonon transport and contribute to the low thermal conductivity. The optimized films, which are achieved at a  $\text{Bi}_2\text{Te}_3$ -deposition rate of  $3.0 \text{ \AA/s}$  and Bi-deposition rate of  $2.0 \text{ \AA/s}$  with a thickness above 100 nm, possess smooth surface of roughness  $< 5.5 \text{ nm}$ , extremely low thermal conductivity of  $0.59 \text{ W/mK}$  and low electrical resistivity of  $3.17 \times 10^{-3} \text{ \Omega cm}$ .

#### CRedit authorship contribution statement

**Yen-Ju Wu:** Investigation. **Shih-Chieh Hsu:** Formal analysis. **Ya-Cheng Lin:** Investigation. **Yibin Xu:** Resources. **Tung-Han Chuang:** Conceptualization, Methodology. **Sheng-Chi Chen:** Conceptualization, Methodology.

#### Declaration of competing interest

The authors declare that they have no known competing financial interests or personal relationships that could have appeared to influence the work reported in this paper.

#### Acknowledgment

We gratefully acknowledge the “Materials research by Information Integration” Initiative (MI2I) project of the Support Program for Starting Up Innovation Hub from Japan Science and Technology Agency (JST) and the Ministry of Science and Technology of Taiwan (No. 107-2221-E-131-036). We also thank Prof. H. C. Lin and Mr. C. Y. Kao of the Instrumentation Center, National Taiwan University for their assistance with EPMA experiments.

#### References

- [1] J.R. Sootsman, D.Y. Chung, M.G. Kanatzidis, New and old concepts in thermoelectric materials, *Angew. Chem. Int. Ed.* 48 (2009) 8616–8639.
- [2] O. Concepcion, M. Galvan-Arellano, V. Torres-Costa, A. Climent-Font, D. Bahena, M. Manso Silvan, A. Escobosa, O. de Melo, Controlling the epitaxial growth of  $\text{Bi}_2\text{Te}_3$ ,  $\text{BiTe}$ , and  $\text{Bi}_4\text{Te}_3$  pure phases by physical vapor transport, *Inorg. Chem.* 57 (2018) 10090–10099.
- [3] H. Cao, R. Venkatasubramanian, C. Liu, J. Pierce, H. Yang, M. Zahid Hasan, Y. Wu, Y.P. Chen, Topological insulator  $\text{Bi}_2\text{Te}_3$  films synthesized by metal organic chemical vapor deposition, *Appl. Phys. Lett.* 101 (2012) 162104.
- [4] S.-D. Kwon, B.-k. Ju, S.-J. Yoon, J.-S. Kim, Fabrication of bismuth telluride-based alloy thin film thermoelectric devices grown by metal organic chemical vapor deposition, *J. Electron. Mater.* 38 (2009) 920–924.
- [5] A. Giani, F. Pascal-Delannoy, A. Boyer, A. Foucaran, M. Gschwind, P. Ancey, Elaboration of  $\text{Bi}_2\text{Te}_3$  by metal organic chemical vapor deposition, *Thin Solid Films* 303 (1997) 1–3.
- [6] X. Wang, H. He, N. Wang, L. Miao, Effects of annealing temperature on thermoelectric properties of  $\text{Bi}_2\text{Te}_3$  films prepared by co-sputtering, *Appl. Surf. Sci.* 276 (2013) 539–542.
- [7] Z.K. Cai, P. Fan, Z.H. Zheng, P.J. Liu, T.B. Chen, X.M. Cai, J.T. Luo, G.X. Liang, D.P. Zhang, Thermoelectric properties and micro-structure characteristics of annealed N-type bismuth telluride thin film, *Appl. Surf. Sci.* 280 (2013) 225–228.
- [8] Z. Zhang, Y. Wang, Y. Deng, Y. Xu, The effect of (001) crystal plane orientation on the thermoelectric properties of  $\text{Bi}_2\text{Te}_3$  thin film, *Solid State Commun.* 151 (2011) 1520–1523.
- [9] L.M. Goncalves, C. Couto, P. Alpuim, A.G. Rolo, F. Völklein, J.H. Correia, Optimization of thermoelectric properties on  $\text{Bi}_2\text{Te}_3$  thin films deposited by thermal co-evaporation, *Thin Solid Films* 518 (2010) 2816–2821.
- [10] L.M. Goncalves, P. Alpuim, G. Min, D.M. Rowe, C. Couto, J.H. Correia, Optimization of  $\text{Bi}_2\text{Te}_3$  and  $\text{Sb}_2\text{Te}_3$  thin films deposited by co-evaporation on polyimide for thermoelectric applications, *Vacuum* 82 (2008) 1499–1502.
- [11] S. Lal, D. Gautam, K.M. Razeeb, Optimization of annealing conditions to enhance thermoelectric performance of electrodeposited p-type  $\text{BiSbTe}$  thin films, *APL Materials* 7 (2019) 031102.
- [12] M. Tan, Y. Hao, G. Wang, Improvement of thermoelectric properties induced by uniquely ordered lattice field in  $\text{Bi}_2\text{Se}_{0.5}\text{Te}_{2.5}$  pillar array, *J. Solid State Chem.* 215 (2014) 219–224.
- [13] M. Tan, Y. Hao, X. Ren, Improvement of thermoelectric properties in  $(\text{Bi}_{0.5}\text{Sb}_{0.5})_2\text{Te}_3$  films of nanolayered pillar arrays, *J. Electron. Mater.* 43 (2014) 3098–3104.
- [14] M. Tan, Y. Deng, Y. Hao, Enhanced thermoelectric properties and superlattice structure of a  $\text{Bi}_2\text{Te}_3/\text{ZrB}_2$  film prepared by ion-beam-assisted deposition, *J. Phys. Chem. C* 117 (2013) 20415–20420.
- [15] A.L. Pires, I.F. Cruz, S. Ferreira-Teixeira, P.M. Resende, A.M. Pereira, Bi-Te thin film produced by ion beam sputtering: impact of beam voltage in the Seebeck coefficient, *Materials Today: Proceedings* 4 (2017) 12383–12390.
- [16] Y. Zhou, L. Li, Q. Tan, J.-F. Li, Thermoelectric properties of Pb-doped bismuth telluride thin films deposited by magnetron sputtering, *J. Alloys Compd.* 590 (2014) 362–367.
- [17] C. Sudarshan, S. Jayakumar, K. Vaideki, C. Sudakar, Effect of vacuum annealing on structural, electrical and thermal properties of e-beam evaporated  $\text{Bi}_2\text{Te}_3$  thin films, *Thin Solid Films* 629 (2017) 28–38.
- [18] P. Nuthongkum, R. Sakdanuphab, Horprathum, Mati, A. Sakulalavek, [bi]:[Te] control, structural and thermoelectric properties of flexible  $\text{Bi}_x\text{Te}_y$  thin films prepared by RF magnetron sputtering at different sputtering pressures, *J. Electron. Mater.* 46 (2017) 6444–6450.
- [19] P.I. Kuznetsov, V.O. Yapaskurt, B.S. Shchamkhalova, V.D. Shcherbakov, G.G. Yakushcheva, V.A. Luzanov, V.A. Jitov, Growth of  $\text{Bi}_2\text{Te}_3$  films and other phases of Bi-Te system by MOVPE, *J. Cryst. Growth* 455 (2016) 122–128.
- [20] A. Fülöp, Y. Song, S. Charpentier, P. Shi, M. Ekström, L. Galletti, R. Arpaia, T. Bauch, F. Lombardi, S. Wang, Phase transition of bismuth telluride thin films grown by MBE, *Appl. Phys. Express* 7 (2014) 045503.
- [21] E.R. Weber, Semiconductors and semimetals, in: T.M. Tritt (Ed.), *Semiconductors and Semimetals*, vol. 71, Elsevier, 2001, p. ii.
- [22] H. Böttner, G. Chen, R. Venkatasubramanian, Aspects of thin-film superlattice thermoelectric materials, devices, and applications, *MRS Bull.* 31 (2006) 211–217.
- [23] M. Martín-González, O. Caballero-Calero, P. Díaz-Chao, Nanoengineering thermoelectrics for 21st century: energy harvesting and other trends in the field, *Renew. Sust. Energy Rev.* 24 (2013) 288–305.
- [24] R. Kato, Y. Xu, M. Goto, Development of a frequency-domain method using completely optical techniques for measuring the interfacial thermal resistance between the metal film and the substrate, *Jpn. J. Appl. Phys.* 50 (2011) 106602.
- [25] X.Y. Wang, H.J. Wang, B. Xiang, H.J. Shang, B. Zhu, Y. Yu, H. Jin, R.F. Zhao, Z.Y. Huang, L.J. Liu, F.Q. Zu, Z.G. Chen, Attaining reduced lattice thermal conductivity and enhanced electrical conductivity in as-sintered pure n-type  $\text{Bi}_2\text{Te}_3$  alloy, *J. Mater. Sci.* 54 (2019) 4788–4797.
- [26] D. Wu, L. Xie, X. Chao, Z. Yang, J. He, Step-up thermoelectric performance realized in  $\text{Bi}_2\text{Te}_3$  alloyed GeTe via carrier concentration and microstructure modulations, *ACS Applied Energy Materials* 2 (2019) 1616–1622.
- [27] M. Goto, M. Sasaki, Y. Xu, T. Zhan, Y. Isoda, Y. Shinohara, Control of p-type and n-type thermoelectric properties of bismuth telluride thin films by combinatorial sputter coating technology, *Appl. Surf. Sci.* 407 (2017) 405–411.
- [28] A.M. Limarga, S. Shian, R.M. Leckie, C.G. Levi, D.R. Clarke, Thermal conductivity of single- and multi-phase compositions in the  $\text{ZrO}_2\text{-Y}_2\text{O}_3\text{-Ta}_2\text{O}_5$  system, *J. Eur. Ceram. Soc.* 34 (2014) 3085–3094.
- [29] T.F. Flint, Y.L. Sun, Q. Xiong, M.C. Smith, J.A. Francis, Phase-field simulation of grain boundary evolution in microstructures containing second-phase particles with heterogeneous thermal properties, *Sci. Rep.* 9 (2019) 18426.
- [30] G.T.-N. Tsao, Thermal conductivity of two-phase materials, *Industrial & Engineering Chemistry* 53 (1961) 395–397.